Version 3.0, 12/22/03

Main Belt Asteroids in Spitzer Observations

This is a brief outline of how to estimate main-belt asteroid counts in Spitzer Space Telescope observations.

There are two physical quantities of interest:

1. Number of asteroids per unit area brighter than a given flux.
2. Typical rates of motion of asteroids at a given solar elongation (to estimate the time needed between multiple observations to identify the source as an asteroid).

Background:

Spitzer will be routinely sensitive to asteroids in the main belt down to a diameter of around D = 0.5 km with the IRAC 8 μm filter and with MIPS at 24 μm. The main-belt asteroid population at this size is not well-determined. Thus we must make an estimate.

Size distribution:

Recent observations have begun to sample the sub-km size distribution of main-belt asteroids. These include results from ISO (Tedesco and Desert 2002), the Sloan Digital Sky Survey (Ivezic *et al.*, 2001), and Suburu (Yoshida *et al.*, 2003). These extend estimates based on the Palomar-Leiden and Spacewatch surveys (e.g. Durda *et al.* 1998). No single power-law fits all of these results. However here we approximate the cumulative size distribution of the main belt with:

$$\mathrm{N}(>\mathrm{D}) = 0.8 \times 10^6 \left(\frac{1}{\mathrm{D}}\right)^{2.0}$$

where D(km) is the asteroid diameter. There is evidence that the power law becomes shallower for asteroids smaller than a few km (Ivezic *et al.* 2001; Yoshida *et al.* 2003). However this approximation should give numbers reliable to within a factor 3 down to 0.3 km.

The Main-Belt simulation:

The positions and fluxes of 9×10^6 main-belt asteroids with diameters larger than D= 0.3 km were simulated with a Monte Carlo model. The distributions of orbital elements a, e, and i of the numbered main-belt asteroids were adopted for the entire sample. The other orbital elements were randomly assigned. This makes the simulation independent of ecliptic longitude, but it ignores the tendency of asteroid perihelion longitudes to fall near Jupiter's (roughly a 40 % effect).

Infrared fluxes were estimated with the standard thermal model for asteroids (Lebofsky and Spencer 1989). The adopted average Bond albedo was A= 0.05. The thermal

emissivity was $\epsilon = 1.0$. The assumed infrared beaming factor was $\eta = 1.2$ (Harris 1998), which may be the most reasonable value for the small bodies of interest here.

Reflected light contributes strongly to the flux in the IRAC 3.6 μm band, moderately at 4.5 μm, and weakly at 5.8 μm. We assume an average geometric albedo of 0.1 (very uncertain) and a phase law like that at visible wavelengths (Bowell *et al.*, 1989).

The main-belt simulation with the adopted power-law and the standard thermal model as described above gives a mid-infrared count rate in the ecliptic plane:

$$\mathrm{N}(> 1 \text{ mJy at } 12\ \mu\mathrm{m}) \quad = \quad 200 \pm 30 \text{ per sq. deg.} \quad \text{(Simulation)}$$

This is higher than the estimate from ISO data of 80 ± 16 (Tedesco and Desert 2002), but it is within a factor 3.

The numbers of asteroids brighter than a given flux limit are given in Table 1 and Figure 1 for a typical Spitzer field-of-view. The flattening of some of the solid lines at low fluxes is due to the low-size cutoff in the simulation. Power-law approximations to the lines before the turnovers, indicated in the figures with dashed lines, can be used to estimate the counts at lower flux levels. But it should be noted that the number of asteroids with sizes below that included in the simulation becomes increasingly uncertain. The raggedness of some of the lines is due to the graininess of the simulation when the number of modelled asteroids becomes relatively small.

Motions:

Rates of motion in ecliptic coordinates from the main-belt simulation are shown in Figure 2 for ecliptic latitudes of 0° and 15°. At a solar elongation of 90°, 99 % of the asteroids move faster than 12 arcsec/hr at an ecliptic latitude of 0°. In order for the majority of asteroids to move more than 1 FWHM of the point spread function, one would have to wait 9.7 and 29 minutes at 8 and 24 μm, respectively (FWHM $\approx \lambda/\mathrm{d}(= 85\mathrm{cm})$). It may be advantageous to allow for several FWHM's of motion.

Credits:

Prepared under the auspices of the Spitzer Science Center by T.Y. Brooke, to whom questions or comments can be addressed: tyb@phobos.caltech.edu. K. Stapelfeldt (JPL) provided software for the main belt asteroid simulation, W. Grundy (Lowell Obs.) provided software for the standard thermal model, and J. Stansberry (U. Ariz.) made helpful comments.

References:

Bowell, E., Hapke, B., Domingue, D., Lumme, K., Peltoniemi, J., and Harris, A. 1989, in *Asteroids II*, ed. R.P. Binzel, T. Gehrels, and M.S. Matthews, Univ. of Ariz. Press, Tucson, p. 524.

Durda, D.D., Greenberg, R., and Jedicke, R. 1998, *Icarus*, **135**, 431.

Harris, A.W. 1998, *Icarus*, **131**, 291.

Ivezic, Z., *et al.* 2001, *AJ*, **122**, 2749.
Lebofsky, L.A. and Spencer, J.R. 1989, in *Asteroids II*, ed. R.T. Binzel, T.Gehrels, and M.S. Matthews, Univ. of Arizona Press, Tucson, p. 128.
Tedesco, E.F. and Desert, F.-X. 2002, *AJ*, **123**, 2070.
Yoshida, F. *et al.* 2003, *PASJ*, **55**, 701.

Table 1
Number of Main Belt Asteroids Brighter than F_ν in a $5' \times 5'$ Area

			IRAC		IRS		MIPS	
λ (μm)	3.6	4.5	5.8	8.0	12	24	70	160
F_ν (mJy)	0.003	0.004	0.02	0.02	0.3	0.1	6.0	50.0
Eclip. Lat.								
0.0	0.94	1.8	2.6	16.8	4.6	27.3	0.18	0.006
2.5	0.77	1.5	2.2	14.5	3.9	22.6	0.14	0.004
5.0	0.44	0.89	1.3	8.5	2.2	12.9	0.08	0.002
7.5	0.20	0.36	0.51	3.5	0.95	5.7	0.04	0.001
10.0	0.11	0.18	0.26	1.8	0.53	3.4	0.02	7.5×10^{-4}
15.0	0.05	0.11	0.15	1.0	0.26	1.5	0.009	2.8×10^{-4}
20.0	0.035	0.097	0.13	0.72	0.17	0.87	0.005	1.5×10^{-4}
25.0	0.020	0.053	0.071	0.41	0.098	0.46	0.002	7.0×10^{-5}
30.0	0.004	0.010	0.013	0.077	0.018	0.091	5.4×10^{-4}	1.6×10^{-5}
45.0	1.0×10^{-4}	3.0×10^{-4}	3.8×10^{-4}	0.002	4.6×10^{-4}	0.002	1.5×10^{-5}	–
60.0	–	–	4.6×10^{-6}	2.4×10^{-5}	–	3.0×10^{-5}	–	–

Note: Asteroid number counts smaller than 1.0×10^{-5} are not shown.

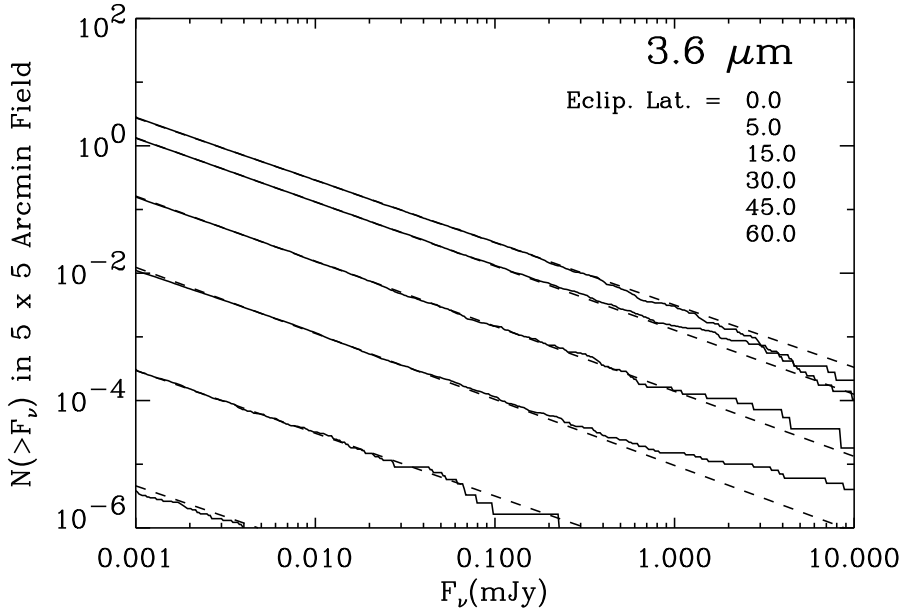

Fig. 1(a) - Simulation of cumulative main-belt asteroids brighter than F_ν in a $5' \times 5'$ area for various ecliptic latitudes at a wavelength of 3.6 μm (solid lines). Also shown are power-law approximations (dashed lines), excluding any regions of turnover due to the lower-size cutoff in the simulation.

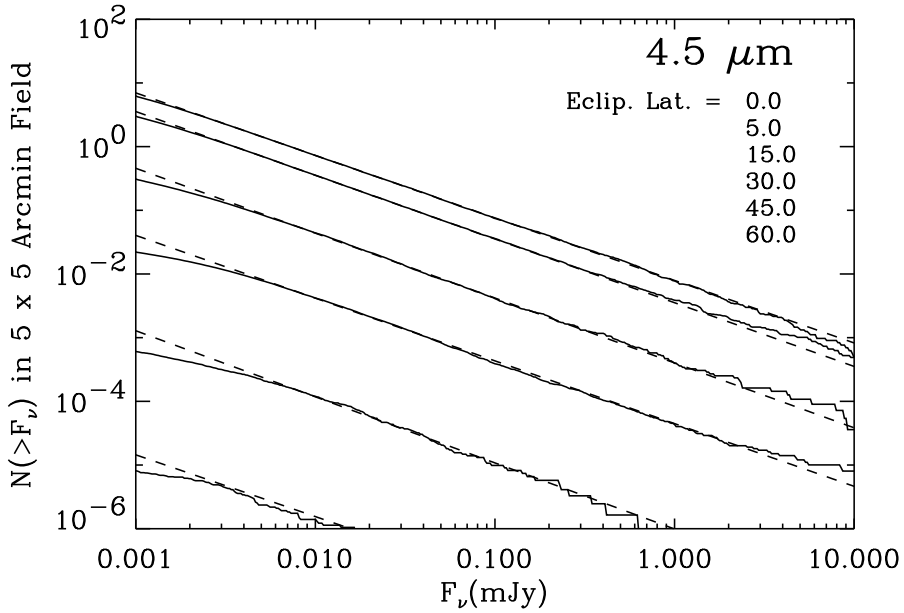

Fig. 1(b) - Same as Fig. 1(a) at 4.5 μm.

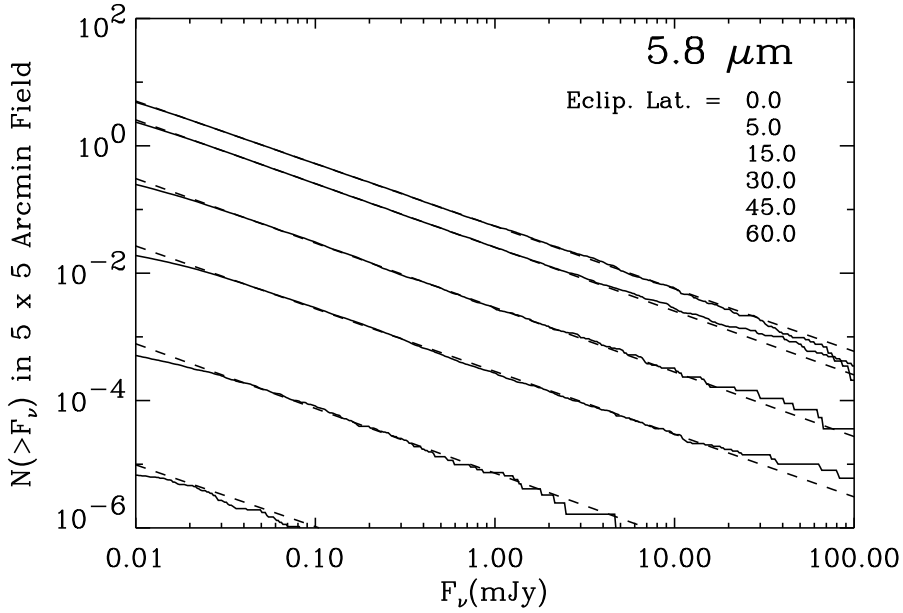

Fig. 1(c) - Same as Fig. 1(a) at 5.8 μm.

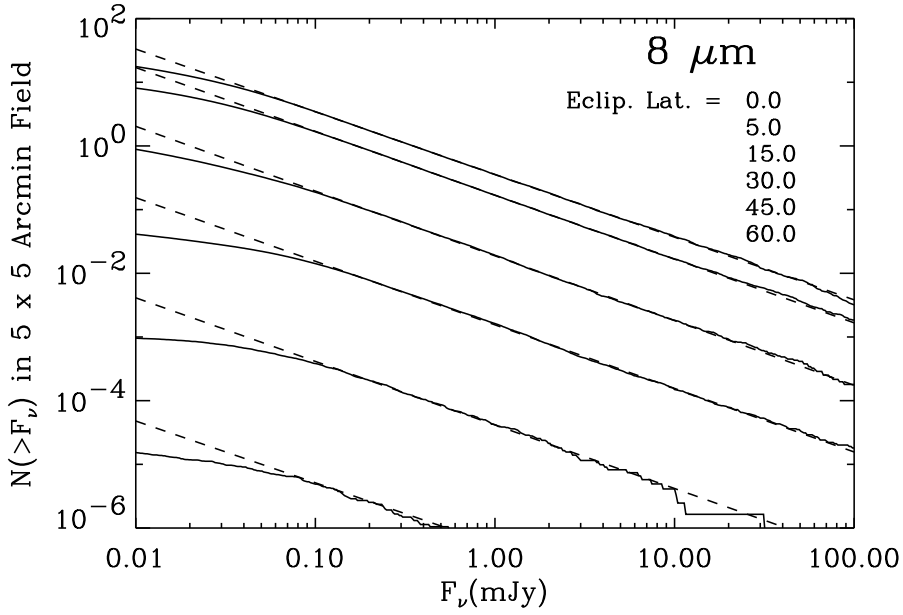

Fig. 1(d) - Same as Fig. 1(a) at 8 μm.

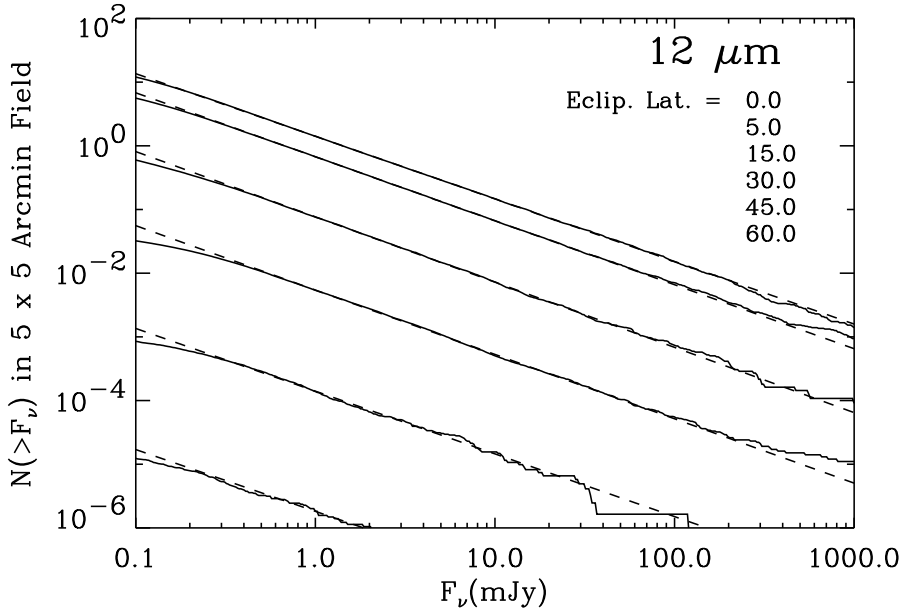

Fig. 1(e) - Same as Fig. 1(a) at 12 μm.

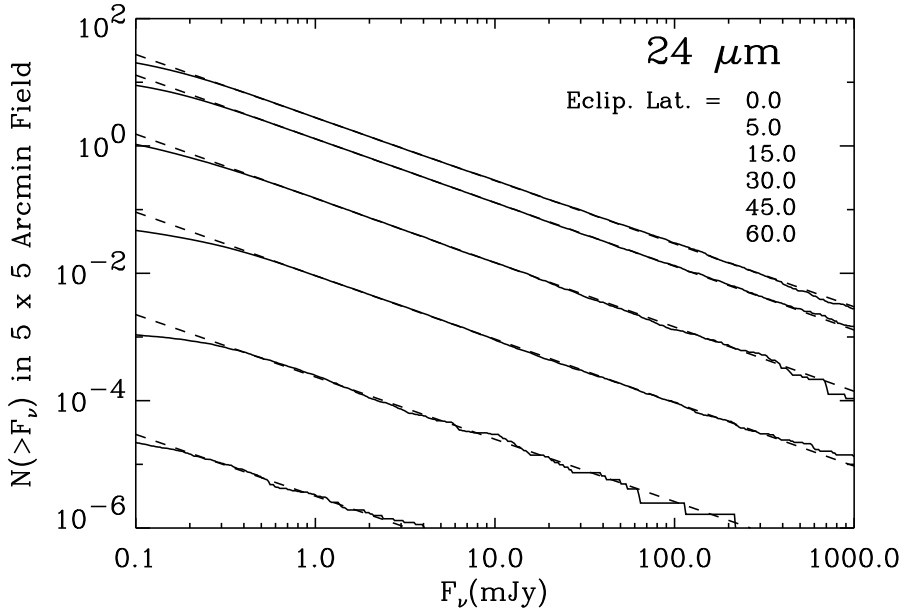

Fig. 1(f) - Same as Fig. 1(a) at 24 μm.

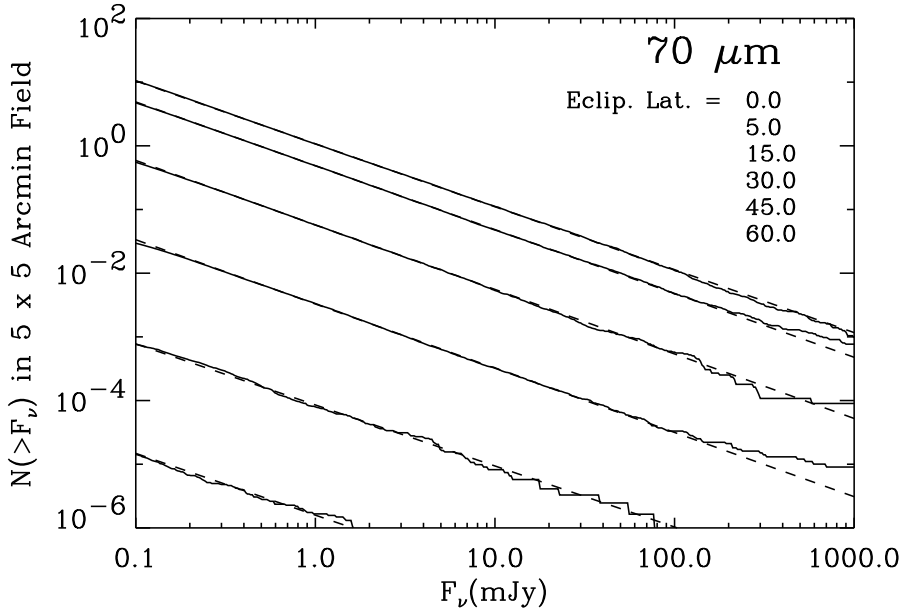

Fig. 1(g) - Same as Fig. 1(a) at 70 μm.

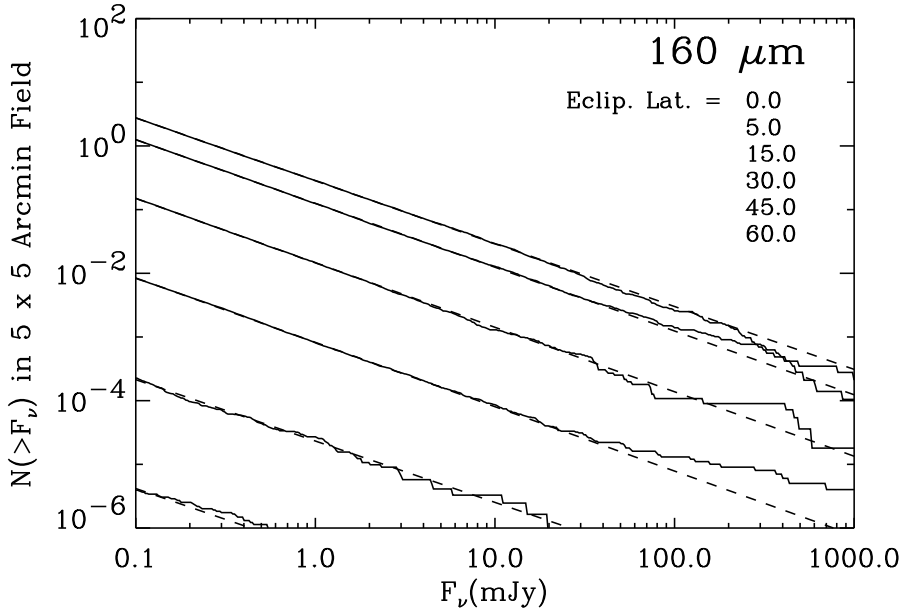

Fig. 1(h) - Same as Fig. 1(a) at 160 μm.

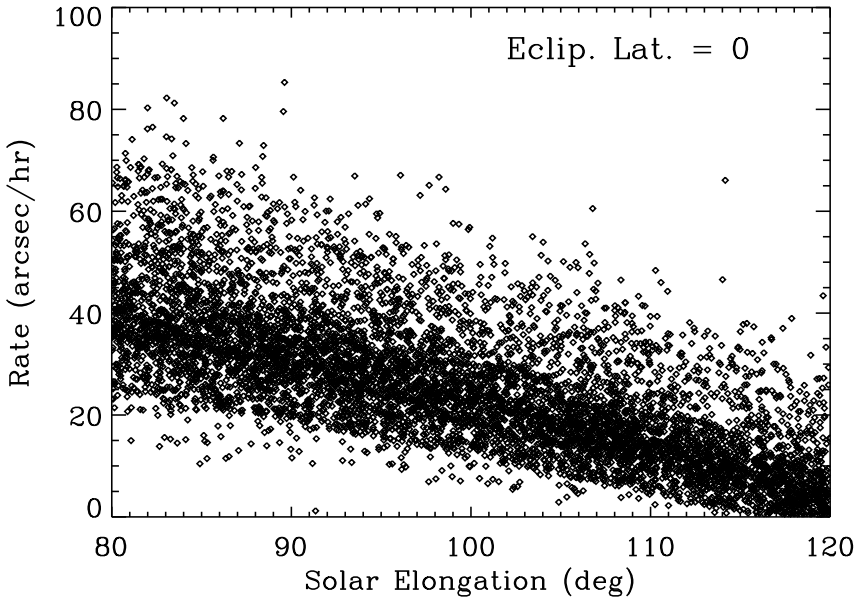

Fig. 2(a) - Simulation of the motions of main-belt asteroids in ecliptic coordinates as a function of solar elongation. Shown are 7500 objects with diameters greater than 1 km in a 0.5°-wide ecliptic latitude bin around 0°.

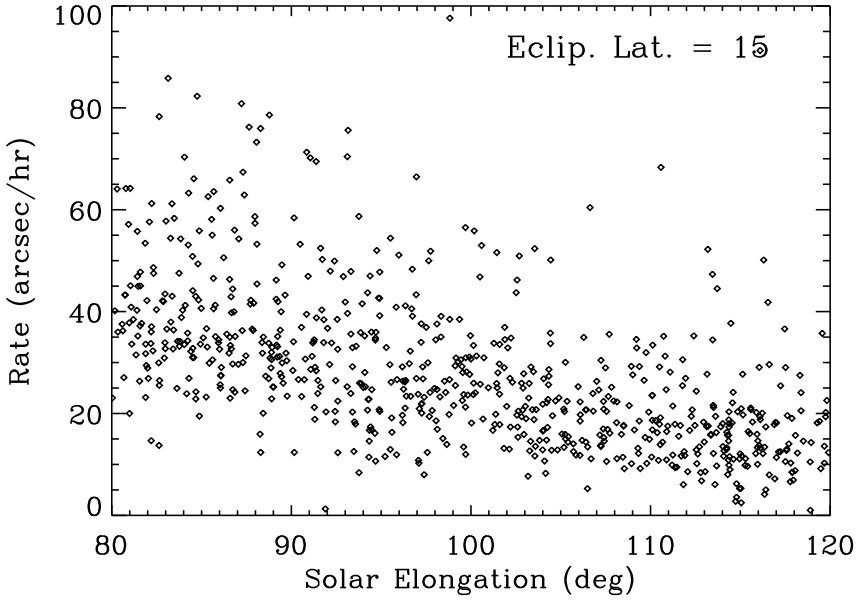

Fig. 2(b) - Same as Fig. 2(a) for 730 objects in two 0.5°-wide ecliptic latitude bins around ±15°.